Langmuir

ARTICLE

pubs.acs.org/Langmuir

Solvent-Induced Helix Superstructure in Achiral Dumbbell-Shaped Hydrazine Derivatives

Xia Ran,[†,§] Peng Zhang,[†,§] Songnan Qu,[‡] Haitao Wang,[†] Binglian Bai,[†] Huimin Liu,[†] Chengxiao Zhao,[†] and Min Li*[,†]

[†]Key Laboratory of Automobile Materials, Ministry of Education, Institute of Materials Science and Engineering, Jilin University, Changchun 130012, People's Republic of China

[‡]Key Laboratory of Excited State Processes, Changchun Institute of Optics, Fine Mechanics and Physics, Chinese Academy of Sciences, Changchun 130033, People's Republic of China

Supporting Information

ABSTRACT: We studied hydrogen-bonding assemblies in a series of dumbbell-shaped hydrazine derivatives, namely oxalyl *N*′,*N*′-bis(3,4-dialkoxybenzoyl)-hydrazide (BFH-*n*, *n* = 4, 6, 8, 10) and oxalyl *N*′,*N*′-dibenzoyl-hydrazide (FH-0). It has been demonstrated that NH-1 protons of BFH-*n* precipitated from tetrahydrofuran (THF) or dimethylformamide (DMF) were involved in intramolecular H-bonding to form 6-membered rings. Meanwhile, NH-2 protons of BFH-*n* precipitated from THF formed intermolecular hydrogen bonds with C═O groups of neighboring molecules, while NH-2 protons of BFH-*n* precipitated from DMF formed intermolecular hydrogen bonds with C═O group of neighboring DMF molecules. C═O, −CH_3, and −CH groups of DMF molecules participated in multiple intermolecular hydrogen bonds with the −N−H and −C═O groups of FH-0 molecules in single-crystals formed in DMF, leading to a double helix morphology with a pitch of 24.2 Å along the *c* direction. Both left- and right-handed helical micrometer-length ribbons with nonuniform helical pitches were observed in an achiral BFH-10 xerogel precipitated from DMF.

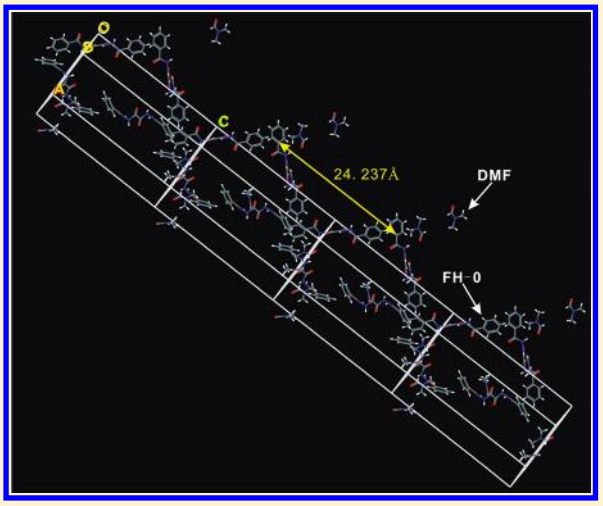

INTRODUCTION

Supramolecular chirality is highly intriguing for its important role in biological phenomena, such as molecular recognition, information storage, and potential applications in materials science.[1] Generally, chiral assemblies are often achieved among chiral molecules or between chiral building blocks.[2] Chirality can also be induced by adding chiral molecules to achiral molecules resulting in various chiral architectures, based on the "sergeants and soldiers principle" and the "majority rules".[3] It is also possible to obtain chiral supramolecular assemblies from achiral molecules. Chiral symmetry breaking from achiral molecules is known to occur in helical supramolecular organization through coordination with metal ions or through hydrogen bonding.[4]

Organogels are the materials in which three-dimensional networks are formed through self-assembly of low-molecular-weight organogelators (LMOGs) through noncovalent interactions, and the network can absorb a large volume of solvent.[5] The formation of an organogel is the result of both gelator−gelator and solvent−gelator interactions, and a gelator only has the ability to induce macroscopic gelation in certain solvents.[6−9] Recently, several detailed studies revealed that solvents play an important role in tuning the morphology of the organogel.[10] For example, Tritt-Goc and co-workers reported that the polarity of the solvent influences the hydrogen-bonding network and the microstructure of the gel network using 1,2-*O*-(1-ethylpropylidene)-α-D-glucofuranose as the gelator,[10h] whereas Shinkai and co-workers reported that the solvent polarity affects the gel microstructure in methyl-4,6-*O*-(*p*-nitrobenzylidene)-α-D-manopyranoside gels, which form helical fibers in water and frizzled fibers in carbon tetrachloride.[10d] Interestingly, helical morphologies can be obtained from achiral organogelators through specific gelator−solvent interactions.[11−13] For example, we reported that both left- and right-handed helical ribbons are formed in the achiral twin-tapered dihydrazide derivatives xerogel from ethanol,[12] whereas You and co-workers reported that a helical nonracemic nanotubular structure is induced by a simple achiral molecule when linked by a linear metal connecting point to form a fibrillar network thereby immobilizing a wide range of

Received: November 3, 2010
Revised: February 21, 2011
Published: March 11, 2011

Scheme 1. Molecular Structures of BFH-*n* and FH-0

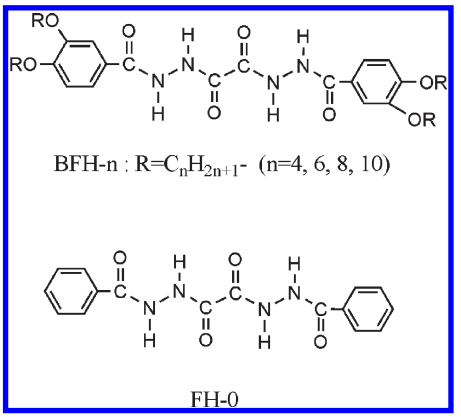

solvents.[13] Although some key points have been recognized, a complete mechanism for the self-assembly of achiral molecules chiral supramolecular structures is still beyond our understanding.

Among the noncovalent interactions, hydrogen bonding is most commonly used to direct self-assembly processes because of its strength, directionality, reversibility, and selectivity. Peptide, amino acid, amide, and urea groups have been widely employed as building blocks to afford supramolecular gels. Wan and co-workers reported a hydrazide quinolinone-based quadruple hydrogen-bonded building block, which can gel dichloromethane/hexane at concentrations higher than 2 wt %.[14] Li and co-workers reported a new series of highly stable hydrazide-based ADDA-DAAD heterodimers, which represented the first successful application of hydrazide derivatives in the self-assembly of hydrogen-mediated supramolecular systems with well-established structures.[15] Herein, we focus on the self-assembly property of a series of achiral dumbbell-shaped molecules, namely oxalyl *N*′,*N*′-bis(3,4-dialkoxybenzoyl)-hydrazide (BFH-*n*, *n* = 4, 6, 8, 10) and oxalyl *N*′,*N*′-dibenzoyl-hydrazide (FH-0) (Scheme 1), which were prepared according to a reported procedure.[16] It was demonstrated that DMF molecules were involved in multiple intermolecular hydrogen bonds with FH-0 molecules in FH-0 single-crystals grown from DMF, leading to a double helix with a pitch of 24.2 Å along the *c* direction. Moreover, left- and right-handed helical micrometer-length ribbons with nonuniform helical pitches were observed in a BFH-10 xerogel precipitated from DMF.

EXPERIMENTAL SECTION

Characterization. ^{1}H NMR spectra were recorded with a Mercury-300BB 300 MHz spectrometer, using tetramethylsilane (TMS) as an internal standard. Field emission scanning electron microscopy (FE-SEM) images were taken with a JSM-6700F apparatus. Samples for FE-SEM measurement were prepared by wiping a small amount of gel onto a silicon plate followed by evaporating the solvent at ambient temperature. X-ray diffraction was carried out with a Bruker Avance D8 X-ray diffractometer. FT-IR spectra were recorded with a Perkin-Elmer spectrometer (Spectrum One B); The xerogels were obtained by freezing and pumping the organogel of BFH-*n* for 12 h, and then the xerogels were pressed into a tablet with KBr for FT-IR measurement.

Gelation test: The weighted gelator was mixed in a capped sealed test tube [3.5 cm (height) × 0.5 cm (radius)] with an appropriate amount of solvent, and the mixture was heated until the solid dissolved. The sample vial was cooled to 4 °C and then turned upside down. When a clear or

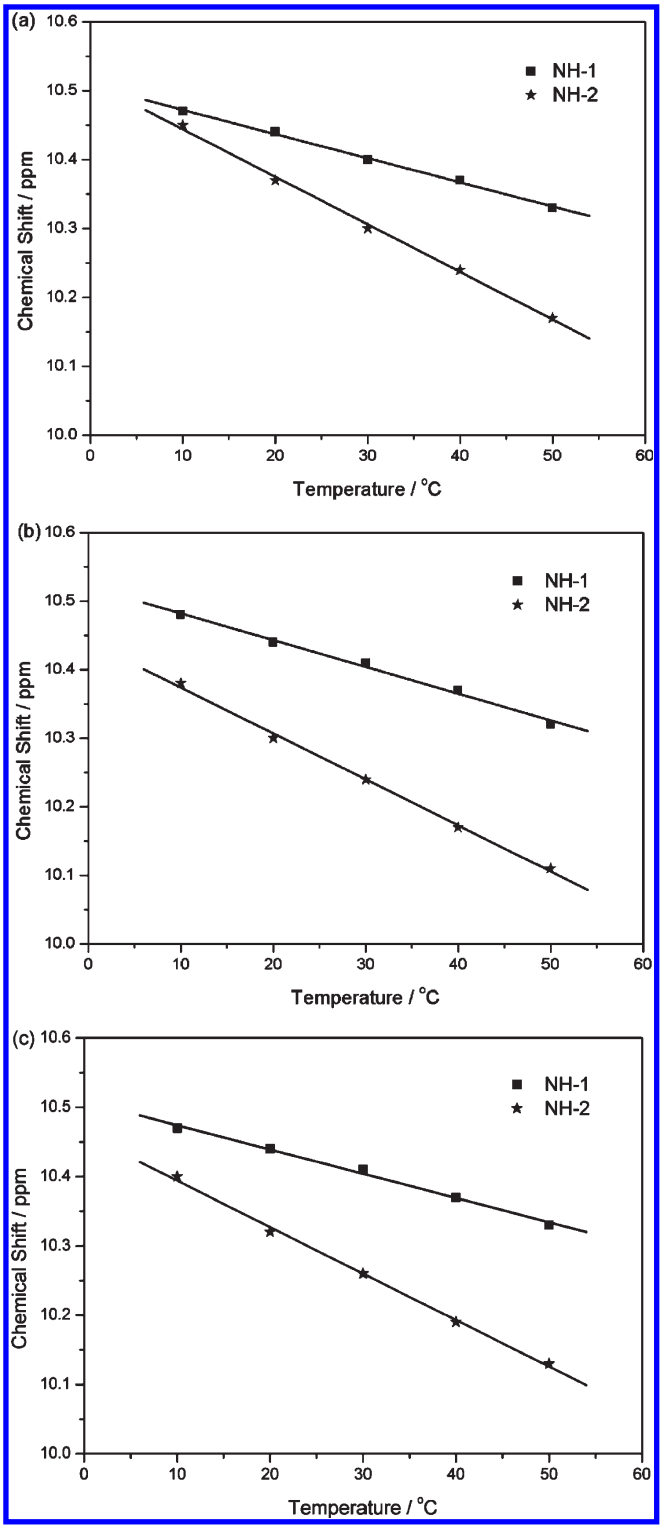

Figure 1. Temperature dependence of chemical shifts of NH-1 and NH-2 of BFH-10 in 20% DMSO-d_6/$CDCl_3$ (a) BFH-10 precipitated (1.87×10^{-3} mol L^{-1}) from THF, (b) BFH-10 precipitated (1×10^{-3} mol L^{-1}) from DMF, and (c) BFH-10 precipitated (1.87×10^{-3} mol L^{-1}) from THF with DMF (3.21×10^{-2} mol L^{-1}) (300 MHz, NH-1: closer to alkoxyphenyl, NH-2: adjacent to central bicarbonyl).

dx.doi.org/10.1021/la104386s |*Langmuir* 2011, 27, 3945–3951

Scheme 2. Hydrogen Bonding Patterns of BFH-*n* in (a) THF and (b) DMF[a]

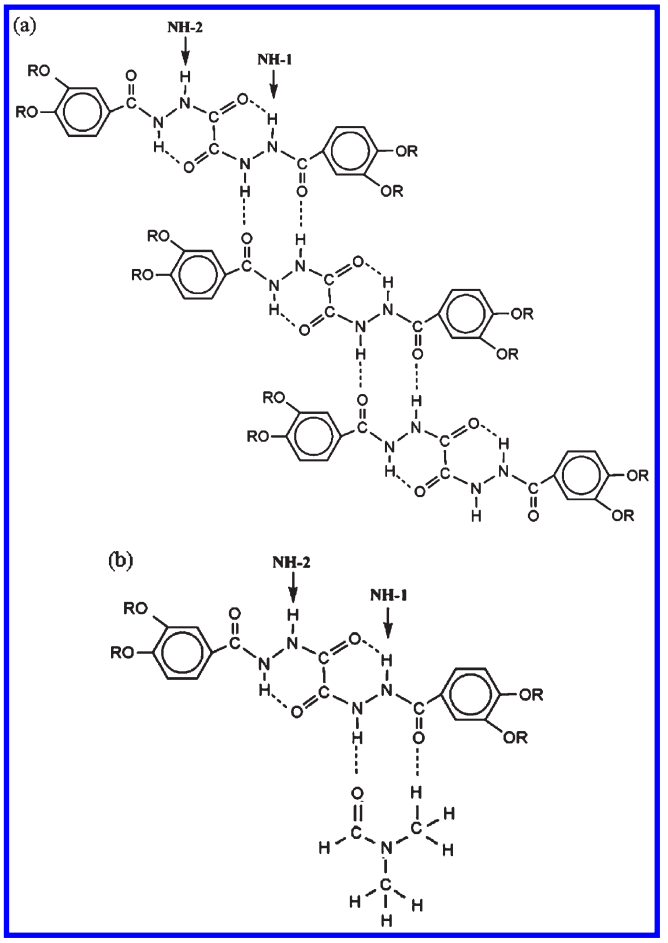

[a] The dashed line illustrates the hydrogen bonding.

slightly opaque gel formed, the solvent therein was immobilized at this stage. Melting temperature (T_m) was determined by the "falling drop" method.[17] An inverted gel was immersed in a water bath initially at or below room temperature. The water bath was heated slowly up to the point at which the gel fell due to the force of gravity, i.e., the T_m.

RESULTS AND DISCUSSION

Hydrogen Bonding in BFH-*n*. Temperature dependent ^{1}H NMR spectroscopic experiments were performed to explore the hydrogen bonding motif in BFH-*n*. Generally, internally hydrogen bonded amides are expected to show a much smaller shift with temperature ($<3.0 \times 10^{-3}$ ppm K^{-1}) compared to those directed externally and accessible for hydrogen bonding to a polar solvent ($>4.0 \times 10^{-3}$ ppm K^{-1}).[18] As shown in Figure 1(a), the NH-2 (adjacent to central bicarbonyl) of BFH-10 precipitated from THF (called BFH-10-THF) showed large shifts (7.0×10^{-3} ppm K^{-1}) with temperature in 20% DMSO-d_6/$CDCl_3$, suggesting the primary involvement of NH-2 protons in intermolecular hydrogen bonding. However, the NH-1 (closer to alkoxyphenyl) showed smaller shifts (3.5×10^{-3} ppm K^{-1}) with temperature, indicating the involvement of NH-1 protons in intramolecular hydrogen bonding. The packing model of BFH-10-THF was proposed in Scheme 2a, in which protons of NH-2 associated with C═O groups of neighboring molecules and

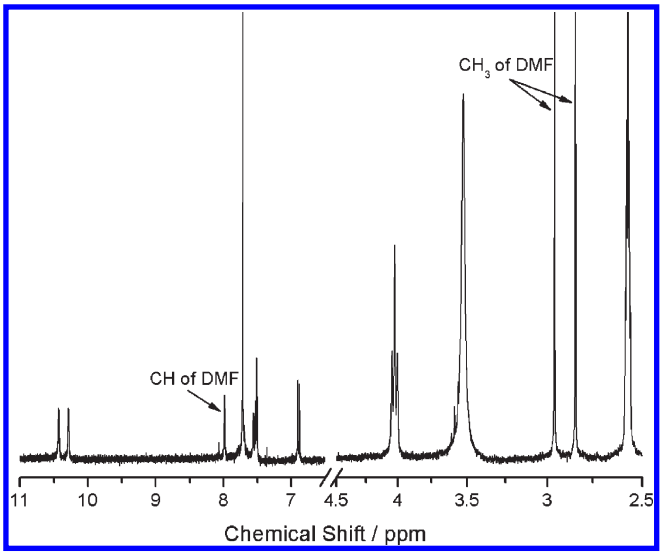

Figure 2. ^{1}H NMR spectrum (δ 2.5−11 ppm region shown; 300 MHz) of BFH-10 precipitated from DMF in 20% DMSO-d_6/$CDCl_3$ at 20 °C.

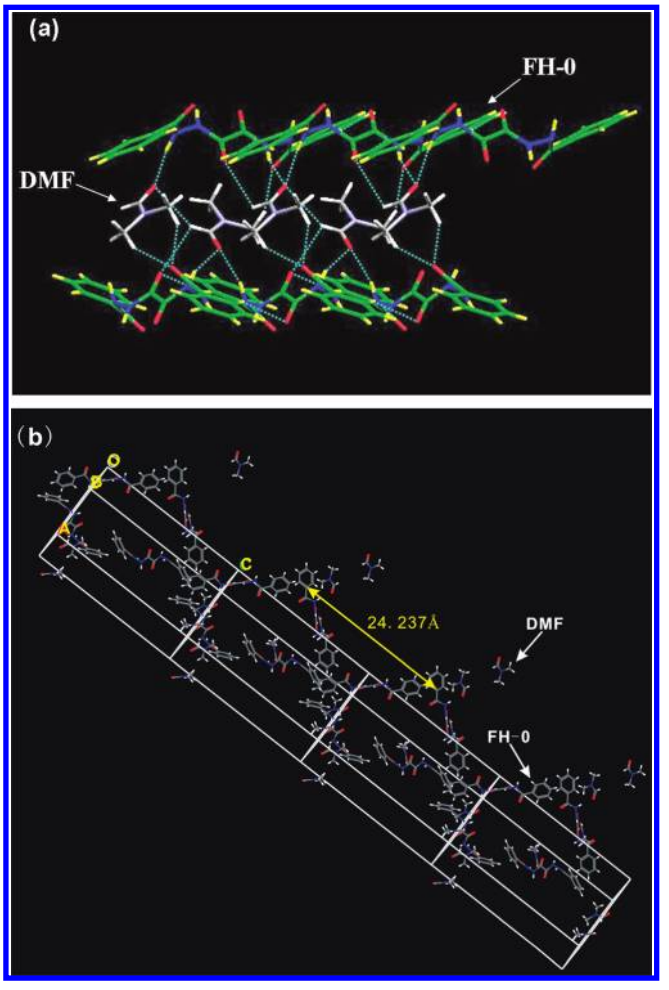

Figure 3. Molecular packing in a single-crystal state: (a) FH-0 and DMF (b) viewed along the *c* axis.

protons of NH-1 were involved in intramolecular hydrogen bonding forming two 6-membered rings.

dx.doi.org/10.1021/la104386s |*Langmuir* 2011, 27, 3945–3951

Table 1. Gelation Properties of BFH-*n* (n = 4, 6, 8, 10)[a]

compound	ethanol	chloroform	DCE	benzene	toluene	DMF	DMSO
BFH-4	I	P	P	P	P	S	S
BFH-6	I	P	P	P	1.19×10^{-2}	S	S
BFH-8	I	P	P	P	2.06×10^{-2}	P	P
BFH-10	I	P	P	P	1.82×10^{-2}	9.93×10^{-3}	P

[a] Values denote the minimum gel concentration (mol L^{-1}) necessary for organogelation. I: insoluble, S: soluble, P: precipitation. DCE, DMF, and DMSO indicate 1,2-dichloroethane, dimethylformamide, and dimethyl sulfoxide.

As shown in Figure 1b, NH-1 and NH-2 of BFH-10 (1×10^{-3} mol L^{-1}) precipitated from DMF (called BFH-10-DMF) showed similar temperature-dependent shifts (3.9×10^{-3} and 6.7×10^{-3} ppm K^{-1}, respectively) with those of BFH-10-THF in 20% DMSO-d_6/$CDCl_3$ in the first heating run. Thus, the NH-1 and NH-2 protons participate in intramolecular and intermolecular hydrogen bonding, respectively, for BFH-10 precipitated either from THF or DMF. The presence of DMF in BFH-10-DMF was confirmed by the ^{1}H NMR spectrum of BFH-10-DMF (Figure 2, in 20% DMSO-d_6/$CDCl_3$; δ of protons in DMF were found at 7.92, 2.89, and 2.78 ppm, respectively).[19] The molar ratio of BFH-10/DMF was calculated to be 1:2 according to the integrated peak area of the protons, which is consistent with the observation in FH-0 single-crystals, suggesting that similar structures might be formed in BFH-10-DMF and FH-0 single crystals. In contrast to that of BFH-10-THF, the characteristic peak of the NH-2 protons of BFH-10-DMF appeared slightly further upfield. Addition of DMF (3.21×10^{-2} mol L^{-1}) to BFH-10-THF in 20% DMSO-d_6/$CDCl_3$ caused a similar upfield shift of NH-2 (Figure 1c), suggesting an interaction between DMF and BFH-10. The temperature-dependences of the chemical shifts of NH-1 and NH-2 of BFH-10 in 20% DMSO-d_6/$CDCl_3$ are quite similar for the first cooling run and the second heating run (Figure S1). Based on the results of ^{1}H NMR spectroscopy, as well as the poor volatility of DMF, it can be concluded that DMF is associated with BFH-*n* in the course of precipitation from DMF.

A packing model of BFH-10 in DMF is shown in Scheme 2b, in which NH-1 protons form two 6-membered rings via intramolecular hydrogen bonding, while NH-2 protons associate with C═O groups of neighboring DMF molecules. In addition, C═O groups of BFH-10 molecules form intermolecular hydrogen bonds with $-CH_3$ groups of DMF molecules.

In order to validate the above hypothesis, FH-0 without terminal alkoxy chains was synthesized by the same method used for BFH-*n*. Single crystals of FH-0, suitable for X-ray analysis were obtained at room temperature from DMF by slow evaporation of the solvent. Crystal data are given in the Supporting Information. DMF molecules interacted with FH-0 molecules in a single-crystal state, as shown in Figure 3a. Protons of N−Hs of FH-0 molecules formed intermolecular hydrogen bonds with C═O groups of DMF molecules (one C═O associated with two N−Hs coming from two different FH-0 molecules). C═O (near to phenyl) groups of FH-0 molecules were involved in intermolecular hydrogen bonding with $-CH_3$ groups of DMF molecules, while one C═O (central bicarbonyl) group of an FH-0 molecule formed an intermolecular hydrogen bond with a C−H group of a DMF molecule and the other C═O was involved in intermolecular hydrogen bonding with a C−H group of a phenyl ring of a neighboring FH-0 molecule. Single crystal analysis indicated that the molar ratio of FH-0/DMF is 1:2. In addition, double helical structures were induced by DMF molecules with a helical pitch of 24.2 Å as seen from the view of the *c* direction (Figure 3b).

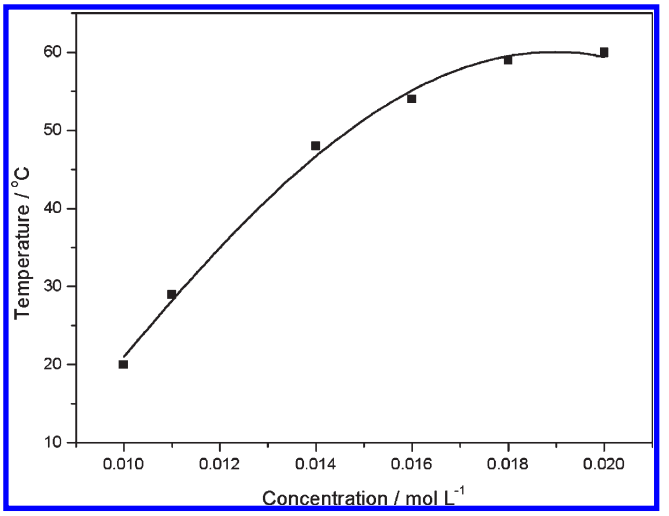

Figure 4. Concentration-dependent melting temperature of BFH-10 gels in DMF.

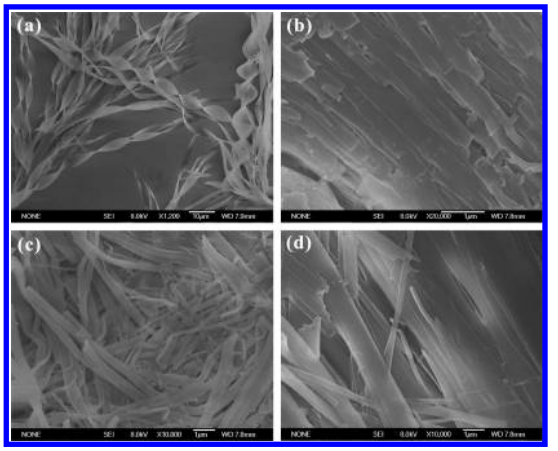

Figure 5. SEM images of xerogels: (a) BFH-10 in DMF (1.2×10^{-2} mol L^{-1}), (b) BFH-10 in toluene (1.9×10^{-2} mol L^{-1}), (c) BFH-8 in toluene (2.2×10^{-2} mol L^{-1}), and (d) BFH-6 in toluene (1.3×10^{-2} mol L^{-1}). The original larger SEM images are included in Supporting Information.

Combining the results of single crystal analysis of FH-0 and the temperature dependent NMR spectroscopic results of BFH-10-DMF, we propose the intermolecular hydrogen bonding motif of BFH-10 from DMF as shown in Scheme 2b. Different from that of BFH-10-THF, NH-2 protons of BFH-10-DMF are H-bonded to C═O groups of DMF resulting in intermolecular H-bonding.

GELATION PROPERTIES

The gelation properties of BFH-*n* were examined for 7 different organic solvents and the minimum gel concentrations are summarized in Table 1. The length of the terminal alkoxy chains clearly affected the gelation ability. Compounds BFH-6, -8, and -10 bearing longer terminal chains can gelate toluene,

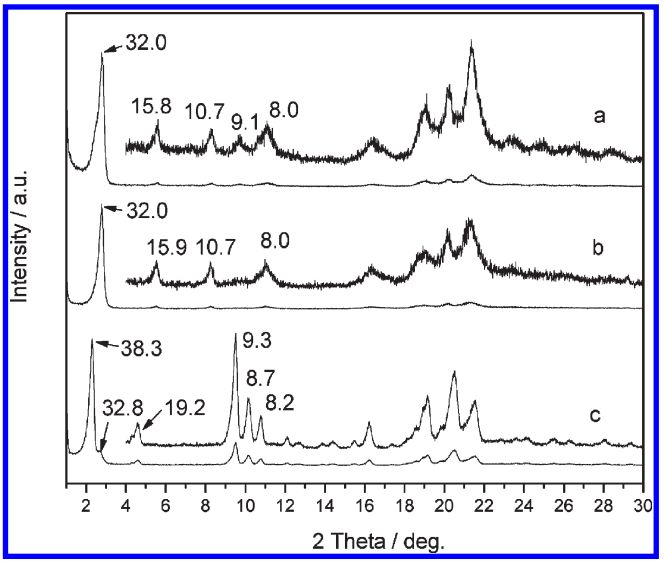

Figure 6. XRD patterns of BFH-10 (a) crystal, (b) xerogel formed from toluene (2.1×10^{-2} mol L^{-1}), and (c) xerogel formed from dimethylformamide (1.8×10^{-2} mol L^{-1}).

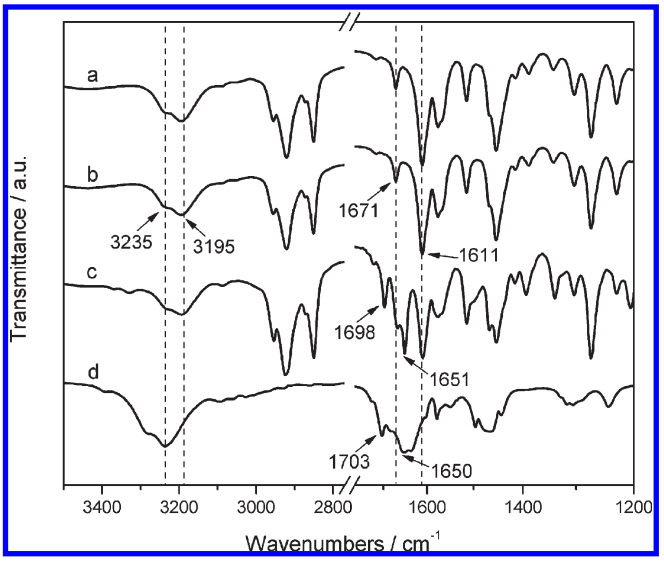

Figure 7. FT-IR spectra of (a) BFH-10 xerogel formed from toluene (1.9×10^{-2} mol L^{-1}), (b) BFH-10 precipitated from THF, (c) BFH-10 xerogel formed from DMF (1.2×10^{-2} mol L^{-1}), and (d) FH-0 single-crystals grown from DMF.

whereas BFH-10 formed a stable gel in DMF. In contrast, compound BFH-4 with shorter terminal chains cannot form a gel in any of the 7 solvents tested. Figure 4 shows the melting temperature (T_m) of a BFH-10 gel in DMF as a function of concentration. T_m values were determined by the falling drop method.[17] The T_m increases from 20 °C for the gel at 1.0×10^{-2} mol L^{-1} to 60 °C at 2.0×10^{-2} mol L^{-1}.

In order to investigate the morphology of these materials, xerogels of BFH-*n* were prepared as described in the Experimental Section and subjected to scanning electron microscopy (SEM). As shown in Figure 5b−d, xerogels of BFH-*n* (n = 6, 8, 10) prepared from toluene consist of flat ribbons 0.2−1.5 μm wide and several tens of micrometers long, indicating that self-

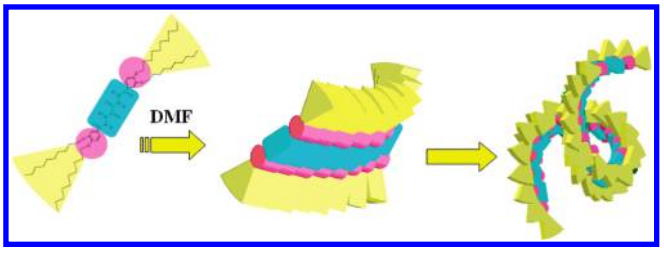

Figure 8. A possible packing motif for BFH-10 xerogel formed from DMF showing helical ribbons.

assembly is driven by strong directional intermolecular interactions. Interestingly, both right- and left-handed helical ribbons with the width of 2−8 μm and ten to hundreds of micrometers in length were observed for a BFH-10 xerogel prepared from DMF (Figure 5a), even though it does not possess any chiral groups. The helical pitches were nonuniform, suggesting that the helical structure did not arise from molecular chirality.

Figure 6 shows X-ray diffraction patterns of BFH-10 crystal and xerogels prepared from toluene and DMF. The XRD pattern of the BFH-10 crystal showed one sharp peak (32.0 Å) and three weak peaks (15.8, 10.7, and 8.0 Å) in the low angle range, suggesting a layered structure. A similar arrangement was observed for the BFH-10 xerogel formed from toluene, indicating a similar supramolecular arrangement in both cases. In contrast, the XRD pattern of the xerogel prepared from DMF was quite different from the others, indicating that the solvent greatly affected the packing modes.

FT-IR spectra of FH-0 single-crystals grown from DMF and BFH-10 xerogels prepared from toluene and DMF were measured (Figure 7). Bands of N−H stretching vibrations of hydrazide groups appear at 3235 and 3195 cm^{-1} as well as amide I bands at 1671 and 1611 cm^{-1}, indicating that the majority of the N−Hs of the hydrazide group are associated with the C═O groups via N−H···*O*═C hydrogen bonding in the xerogel and BFH-10 precipitated from THF (Figure 7, panels a and b), which are involved in intramolecular and intermolecular hydrogen bonding.[20−22] Two new absorption bands for the BFH-10 xerogel formed from DMF appear at 1698 and 1651 cm^{-1} (Figure 7c): these are assigned to the free and associated C═O stretching vibration of DMF in the BFH-10 xerogel, respectively. This assignment is further supported by the observation of bands of the C═O stretching vibration of DMF at 1703 cm^{-1} (free) and 1650 cm^{-1} (H-bonded) in an FH-0 single crystal grown from DMF (Figure 7d). The ^{1}H NMR spectrum of the xerogel formed from DMF (Figure S4) further confirms the presence of the DMF molecules ($CDCl_3$; δ of protons in DMF at 8.01, 2.93, and 2.87 ppm, respectively).[19]

Combining the results of single crystal analysis of FH-0, SEM, FT-IR spectroscopy and ^{1}H NMR spectroscopy of the xerogel, a possible packing motif for BFH-10 molecules in the xerogel formed from DMF and the mechanism for the formation of helical ribbons are illustrated in Figure 8. In this model, BFH-10 molecules rotate to form a twisting supramolecular array through intermolecular hydrogen bonding between BFH-10 and DMF, as well as van der Waals interaction between alkyl chains. N−H protons of BFH-10 molecules form intermolecular hydrogen bonds with C═O groups of neighboring DMF molecules. Meanwhile, C═O groups of BFH-10 molecules are involved in intermolecular hydrogen bonding with $-CH_3$ groups of DMF molecules. Hydrogen-bonding interactions between DMF and

dx.doi.org/10.1021/la104386s |*Langmuir* 2011, 27, 3945–3951

the gelator play an important role in the formation of helical ribbons of the BFH-10 xerogel prepared from DMF. During gelation, DMF molecules penetrate into the twisted molecular arrays, which are sustained by the weak van der Waals interactions between alkyl chains in adjacent screwed arrays. Balancing the stresses in the separated mono or multiple screwed molecular arrays might then give rise to the helical ribbons. More detailed investigation of microscale helical ribbons in BFH-10 gels from DMF is currently in progress.

CONCLUSION

It has been demonstrated that the NH-1 protons of BFH-*n* precipitated from either THF or DMF form intramolecular H-bonded 6-membered rings. While the corresponding NH-2 protons of BFH-*n* precipitated from THF form intermolecular hydrogen bonds with C═O groups of neighboring BFH-*n* molecules, the NH-2 protons of BFH-*n* precipitated from DMF form intermolecular hydrogen bonds with C═O groups of DMF molecules. Single crystal analysis of FH-0 shows that the C═O, $-CH_3$, and −CH groups of DMF molecules form multiple intermolecular hydrogen bonds with the −N−H and −C═O groups of neighboring FH-0 molecules. A double helix with a pitch of 24.2 Å along the *c* direction is observed in the FH-0 single crystal grown from DMF. Furthermore, left- and right-handed helical micrometer-length ribbons with nonuniform helical pitches were observed in a xerogel formed by the achiral BFH-10 precipitated from DMF, which demonstrates that intermolecular hydrogen-bonding interactions between DMF and the gelator play an important role in the formation of helical ribbons of BFH-10 xerogel prepared from DMF. This new self-assembly of dumbbell-shaped molecules containing hydrazide units offers excellent opportunities for the organization of other functional groups.

ASSOCIATED CONTENT

Supporting Information. Synthesis and characterization of BFH-*n* (*n* = 4, 6, 8, 10) and FH-0. Partial proton NMR spectra for NH-1 and NH-2 of BFH-10-DMF in the first heating run, the first cooling run and the second heating run for BFH-10-THF and BFH-10-THF with DMF in 20% DMSO-d_6/$CDCl_3$ versus temperature (300 MHz). FT-IR spectra of BFH-*n* (*n* = 6, 8, 10) xerogels prepared from toluene. X-ray diffraction pattern of FH-0 single-crystals grown from DMF. The ^{1}H NMR spectrum of the BFH-10 xerogel formed from DMF. Single crystal data of FH-0. CCDC reference number for FH-0 CCDC 799280. Original larger SEM images of Figure 5a−d. This material is available free of charge via the Internet at http://pubs.acs.org.

AUTHOR INFORMATION

Corresponding Author

*E-mail: minli@mail.jlu.edu.cn. Fax: 86 431 85168444.

Author Contributions

§Peng Zhang contributed with Xia Ran, and they are both the first author.

ACKNOWLEDGMENT

The authors are grateful to the National Science Foundation Committee of China (Project Nos. 50873044, 51073071, and 21072076), and Project 985-Automotive Engineering of Jilin University for their financial support of this work.

REFERENCES

(1) (a) Lough, W. J.; Wainer, I. W. *Chirality in Nature and Applied Science*; CRC Press: Oxford, U.K., 2002. (b) Cornelissen, J. J. L. M.; Rowan, A. E.; Nolte, R. J. M.; Sommerdijk, N. A. J. M. *Chem. Rev.* **2001**, *101*, 4039. (c) Perez-Garcia, L.; Amabilino, D. B. *Chem. Soc. Rev.* **2002**, *31*, 342. (d) Mateos-Timoneda, M. A.; Crego- Calama, M.; Reinhoudt, D. N. *Chem. Soc. Rev.* **2004**, *33*, 363. (e) Link, D. R.; Natale, G.; Shao, R.; Maclennan, J. E.; Clark, N. A.; Korblova, E.; Walba, D. M. *Science* **1997**, *278*, 1924. (f) Heppke, G.; Moro, D. *Science* **1998**, *279*, 1872. (g) Simonyi, M.; Bikdi, Z.; Zsila, F.; Deli, J. *Chirality* **2003**, *15*, 680. (h) Surez, M.; Branda, N.; Lehn, J.-M.; Decian, A.; Fischer, J. *Helv. Chim. Acta* **1998**, *81*, 1.

(2) (a) Rowan, A. E.; Nolte, R. J. M. *Angew. Chem., Int. Ed.* **1998**, *37*, 63. (b) Hirschberg, J. H. K. K.; Brunsveld, L.; Ramzi, A.; Vekemans, J. A. J. M.; Sijbesma, R. P.; Meijer, E. W. *Nature* **2000**, *407*, 167.

(3) (a) Palmans, A. R. A.; Meijer, E. W. *Angew. Chem., Int. Ed.* **2007**, *46*, 8948. (b) Green, M. M.; Park, J.-W.; Sato, T.; Teramoto, A.; Lifson, S.; Selinger, R. L. B.; Selinger, J. V. *Angew. Chem., Int. Ed.* **1999**, *38*, 3138. (c) Green, M. M.; Cheon, K.-S.; Yang, S.-Y.; Park, J.-W.; Swansburg, S.; Liu, W. *Acc. Chem. Res.* **2001**, *34*, 672. (d) Yashima, E.; Maeda, K.; Nishimura, T. *Chem.−Eur. J.* **2004**, *10*, 42.

(4) (a) Wu, S.-T.; Wu, Y.-R.; Kang, Q.-Q.; Zhang, H.; Long, L.-S.; Zheng, Z.; Huang, R.-B.; Zheng, L.-S. *Angew. Chem., Int. Ed.* **2007**, *46*, 8475. (b) Yuan, J.; Liu, M. *J. Am. Chem. Soc.* **2003**, *125*, 5051. (c) Ezuhara, T.; Endo, K.; Aoyama, Y. *J. Am. Chem. Soc.* **1999**, *121*, 3279.

(5) (a) Terech, P.; Weiss, R. G. *Chem. Rev.* **1997**, *97*, 3133. (b) Esch, J.; Feringa, B. L. *Angew. Chem., Int. Ed.* **2000**, *39*, 2263.

(6) Zhu, G. Y.; Dordick, J. S. *Chem. Mater.* **2006**, *18*, 5988.

(7) Hanabusa, K.; Matsumoto, M.; Kimura, M.; Kakehi, A.; Shirai, H. J. *Colloid Interface Sci.* **2000**, *224*, 231.

(8) Hirst, A. R.; Smith, D. K. *Langmuir* **2004**, *20*, 10851.

(9) John, G.; Jung, J. H.; Masuda, M.; Shimizu, T. *Langmuir* **2004**, *20*, 2060.

(10) (a) Luboradzki, R.; Pakulski, Z.; Sartowska, B. *Tetrahedron* **2005**, *61*, 10122. (b) Luboradzki, R.; Pakulski, Z. *Tetrahedron* **2004**, *60*, 4613. (c) Gronwald, O.; Sakurai, K.; Luboradzki, R.; Kiura, T.; Shinkai, S. J. *Carbohydr. Res.* **2001**, *331*, 307. (d) Gronwald, O.; Shinkai, S. J. *Chem. Soc., Perkin Trans.* **2001**, *2*, 1933. (e) Suzuki, A.; Yumoto, M.; Kimura, M.; Shirai, H.; Hanabusa, K. *Chem. Commun.* **2002**, *8*, 884. (f) Amanokura, N.; Kanekiyo, Y.; Shinkai, S. J.; Reinhoudt, D. N. J. *Chem. Soc., Perkin Trans.* **1999**, *2*, 1995. (g) Suzuki, M.; Nakajima, Y.; Sato, T.; Shirai, H.; Hanabusa, K. *Chem. Commun.* **2006**, *4*, 377. (h) Bielejewski, M.; Lapinshi, A.; Luboradzki, R.; Tritt-Goc, J. *Langmuir* **2009**, *25*, 8274.

(11) (a) Bao, C.; Lu, R.; Jin, M.; Xue, P.; Tan, C.; Xu, T.; Liu, G.; Zhao, Y. *Chem.−Eur. J.* **2006**, *12*, 3287. (b) van Esch, J.; Feyter, S. D.; Kellogg, R. M.; Schryver, F. D.; Feringa, B. L. *Chem.−Eur. J.* **1997**, *3*, 1238. (c) Dumitru, F.; Legrand, Y. M.; Lee, A. V.; Barboiu, M. *Chem. Commum.* **2009**, 2667.

(12) (a) Qu, S. N.; Zhao, L. J.; Yu, Z. X.; Xiu, Z. Y.; Zhao, C. X.; Zhang, P.; Long, B. H.; Li, M. *Langmuir* **2009**, *25*, 1713. (b) Qu, S. N.; Wang, H. T.; Yu, Z. X.; Bai, B. L.; Li, M. *New J. Chem.* **2008**, *32*, 2023.

(13) Zhang, S. Y.; Yang, S. Y.; Lan, J. B.; Yang, S. J.; You, J. S. *Chem. Commum.* **2008**, 6170.

(14) Yang, Y.; Yan, H. J.; Chen, C. F.; Wan, L. J. *Org. Lett.* **2007**, *9*, 4991.

(15) Zhao, X.; Wang, X.-Z.; Jiang, X.-K.; Chen, Y.-Q.; Li, Z.-T.; Chen, G.-J. *J. Am. Chem. Soc.* **2003**, *125*, 15128.

(16) Zhang, P.; Qu, S. N.; Bai, B. L.; Wang, H. T.; Ran, X.; Zhao, C. X.; Li, M. *Liq. Cryst.* **2009**, *36*, 817.

(17) Abdallah, D. J.; Weiss, R. G. *Langmuir* **2000**, *16*, 352.

(18) (a) Hamuro, Y.; Geib, S. J.; Hamilton, A. D. *J. Am. Chem. Soc.* **1996**, *118*, 7529. (b) Hamuro, Y.; Geib, S. J.; Hamilto, A. D. *J. Am. Chem. Soc.* **1997**, *119*, 10587.

(19) Gottlieb, H. E.; Kotlyar, V.; Nudelman, A. *J. Org. Chem.* **1997**, *62*, 7512.
(20) Pang, D. M.; Wang, H. T.; Li, M. *Tetrahedron* **2005**, *61*, 6108.
(21) Qu, S. N.; Li, F.; Wang, H. T.; Bai, B. L.; Xu, C. Y.; Zhao, L. J.; Long, B. H.; Li, M. *Chem. Mater.* **2007**, *19*, 4839.
(22) (a) Xue, C.; Jin, S.; Weng, X.; Ge, J. J.; Shen, Z.; Shen, H.; Graham, M. J.; Jeong, J. K.; Huang, H.; Zhang, D.; Guo, M.; Harris, F. W.; Cheng, S. Z. D. *Chem. Mater.* **2004**, *16*, 1014. (b) Shen, H.; Jeong, J. K.; Xiong, H.; Graham, M. J.; Leng, S.; Zheng, J. X.; Huang, H.; Guo, M.; Harris, F. W.; Cheng, S. Z. D. *Soft Matter* **2006**, *2*, 232.